A R C H I V E S O F M E T A L L U R G Y A N D M A T E R I A L S
Volume 54 2009 Issue 2

K. BANAŚ*, J. BANAŚ**

CORROSION BEHAVIOR OF LOW CHROMIUM Fe-Cr ALLOYS IN ANHYDROUS METHANOL SOLUTIONS OF SULFURIC ACID

KOROZYJNE WŁAŚCIWOŚCI NISKOCHROMOWYCH STOPÓW Fe-Cr W BEZWODNYCH METANOLOWYCH ROZTWORACH KWASU SIARKOWEGO

The research presents the influence of a little amount of chromium in ferritic Fe-Cr alloys on their electrochemical and corrosive properties in anhydrous CH_3OH-0.1M H_2SO_4 solution. In this environment iron and investigated alloys are subject to corrosion in the active range. The research presents the mechanism of corrosion and the influence of chromium on the cathodic reduction of hydrogen ions and anodic oxidation of alloy. The presence of a little amount of chromium in ferrite stimulates hydrogen evolution and inhibits anodic dissolution of metal. The formation of intermediate surface $CrOCH_3$ compounds affects electrochemical reactions at low overvoltage.

W pracy przedstawiono wpływ niewielkich ilości chromu w ferrytycznych stopach Fe-Cr na ich własności elektrochemiczne i korozyjne w bezwodnym roztworze CH_3OH-0.1M H_2SO_4. Żelazo i badane stopy ulegają w tych warunkach korozji w zakresie aktywnym. Przedstawiono mechanizm korozji oraz wpływ chromu na reakcję katodowego wydzielania wodoru i anodowego roztwarzania stopu. Obecność już niewielkich ilości chromu w stopach żelaza stymuluje wydzielanie wodoru i inhibituje anodowe roztwarzanie metalu. Przyczyną tego zjawiska jest obecność powierzchniowego produktu $CrOCH_3$ na powierzchni stopu.

1. Introduction

Research of the electrochemical and corrosion properties of metals in anhydrous methanol solutions has significant scientific and practical importance. Practical aspect is connected with the use of methanol in numerous technological processes and the growing importance of this compound as a fuel. Methanol is the simplest alcohol thus its electrochemical research can lead to interesting conclusions.

Iron is not subject to passivation in diluted methanol solutions of oxy-acids [1,2,3]. Transition into passive state is possible only in the presence of free water particles. It takes place when the ratio H^+/H_2O is lower than $^1/_4$. At the higher ratio strong bonding of four water particles by H^+ ion eliminates practically water activity [2]. Methanol particles are not the source of oxygen in the process of oxygen formation. The water molecules or undissociated particles of oxy-acids (e.g. H_2SO_4, HCOOH) are necessary for the formation of passive film. In the second case the growth of the oxygen layer is accompanied by electro- catalytic decomposition of acid particle similar as it takes place in concentrated solutions with oxidizing properties. [3,4].

Iron corrosion in diluted anhydrous methanol solutions of acids proceeds in the active range with hydrogen depolarization [4-9]. Cathodic reduction of hydrogen ions in methanol solutions is limited by " ion – atom" Heyrowski mechanism with the Tafel slope $dE/d\log i$ = -0.118 V [9]. Little is known about the mechanism of anodic reaction in this environment and especially about the role of the methanol particles in the ionization of metal. The participation of methanol particles in anodic process and the presence of $Fe(OCH_3)_2$ product on the surface of iron have been only proved for the neutral methanol solutions of lithium perchlorate [10,11].

The presence of hydrogen ions in anhydrous methanol stimulates the activation of the metal surface and therefore the inhibiting role of methoxide film decreases at the growth of the concentration of hydrogen ions [11]. The presence of complexing ions or parti-

* FACULTY OF NON-FERROUS METALS, AGH UNIVERSITY OF SCIENCE AND TECHNOLOGY, 30-059 KRAKÓW, 30 MICKIEWICZA AV., POLAND
** FACULTY OF FOUNDRY ENGINEERING, AGH UNIVERSITY OF SCIENCE AND TECHNOLOGY, 30-059 KRAKÓW, 23 REYMONTA STR., POLAND

cles in methanol leads to the replacement of methoxy groups in anodic reaction and formation of soluble Fe^{2+} complex [12]. That is why anodic dissolution of iron in anhydrous CH_3OH-HCl proceeds with participation of chloride ions. The mechanism and kinetics of this process was presented by Sternberg and Brânzoi [5]. Little is known about mechanism and kinetics of anodic reaction on iron surface in acid methanol solutions without the presence of complexing anions, e.g. in methanol solutions of sulfuric acid.

Anodic behavior of chromium in active range in anhydrous methanol solutions of electrolytes is completely unknown. All former research of anodic behavior of chromium and Fe-Cr alloys in methanol solutions were focused only on the passivation mechanism and on the role of chromium in the formation of oxide film on Fe-Cr alloys. [13-15]. Polarization curves of chromium in anhydrous solutions of CH_3OH-H_2SO_4 indicate active – passive transition [13] and the presence of this element in Fe-Cr alloys stimulates their passivation in anhydrous organic solutions of sulfuric acid similar to how it takes place in water media [15]. Mechanism of passivation in anhydrous solutions of sulfuric acid is hoverer different than in water solutions and takes place with participation of H_2SO_4 particles and not the solvent molecules [2-4,17,18]. Chromium as the element of high oxygen affinity stimulates this process.

The aim of this research was to investigate the influence of small chromium amount in ferrite on its electrochemical behavior in CH_3OH – 0.1M H_2SO_4, in environment where passivation of low chromium iron alloys does not take place. In such conditions Fe-Cr alloys are subject to corrosion in the active range.

2. Experimental

The measurements were made on iron of spectral purity and on two – component Fe-Cr alloys having the content and thermal treatment as illustrated in Table 1. The aim of thermal treatment (solution annealing) was to reach possibly pure ferrite structure. Figure 1 presents microstructure of investigated alloys after heat treatment. Electrochemical research was done in argon purged anhydrous solution of CH_3OH – 0.1M H_2SO_4 at the temperature of 20°C. Solutions were made from dehydrated methanol with the use of Bjerrum method [19] and 98% H_2SO_4. Residual amount of water was bound with the help of oleum. Samples for the research in teflon holder, having active surface of 0.5 cm^2, were mechanically polished with sand papers up 1000, washed in methanol with ultrasound washer and dried in the stream of air.

TABLE 1

Chemical content (wt %) and thermal treatment of Fe-Cr alloys

Alloy	C	Si	Mn	P	S	Cr	Ni	Mo	Cu	Thermal treatment
Fe1%Cr	0.03	0.01	0.131	0.012	0.011	0.87	0.019	<0.0007	0.0420	11000C/100h/argon
Fe3%Cr	0.03	0.01	0.132	0.013	0.012	2.80	0.018	<0.0007	0.0366	11000C/100h/argon
Fe5%Cr	0.03	0.03	0.126	0.021	0.015	5.16	0.020	<0.0012	0.0314	11000C/100h/argon

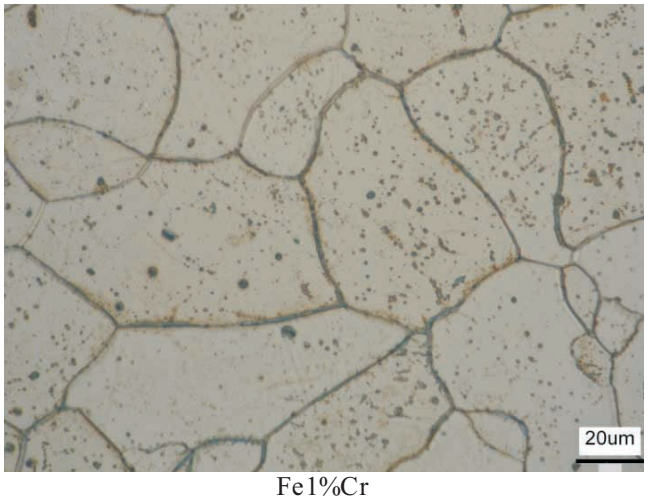

Fe1%Cr

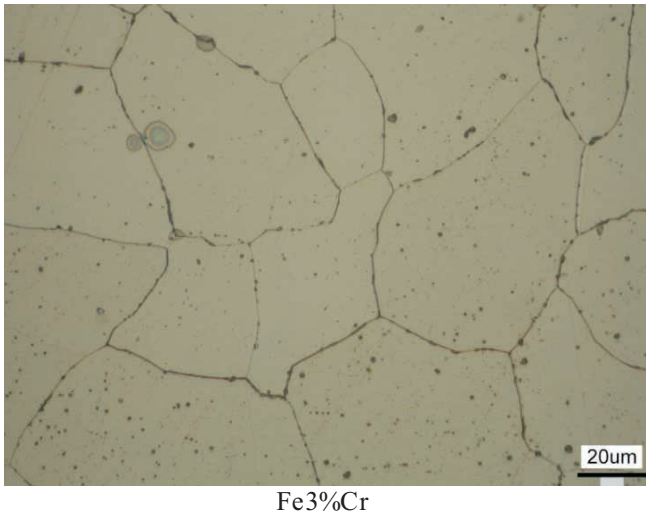

Fe3%Cr

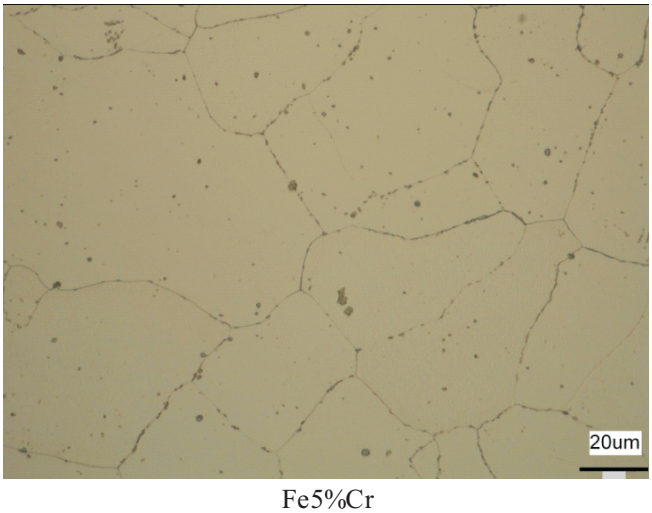

Fe5%Cr

Fig. 1. Microstructure of the Fe-Cr alloys

Voltamperometric (LSV) and impedance (EIS) measurements were performed with the use of ATLAS 0531 electrochemical station. Voltamperometric curves were drawn with the scan rate of 1,3,5,10, and 20 V/min, versus standard hydrogen electrode. Three consecutive runs were made from the potential about -2V to about 0 V. At the high densities of current there was visible linear dependence of current on potential, on voltamperometric curves, which is the result of resistance control of polarization (Fig 2.). The slope of linear sections of

polarization curves is the same for anodic and cathodic branches and does not depend on the scan rate (Fig.3). It enables to calculate electrolyte resistance between Luggin capillary and electrode and to correct polarization curves by the *IR* drop. Fig.2 to Fig.4 show the process of the correction of polarization curves.

TABLE 2

Parameters of equivalent circuit R(CR)(C(LR)(LR))

Stop	R_{e1} Ω cm^2	C_e F/cm^2	R_{e2} Ω cm^2	C_{dl} F/cm^2	L_1 H	R_1 Ω cm^2	L_2 H	R_2 Ω cm^2	R_{ct} Ω cm^2	$R_{e1} + R_{e2}$ Ω cm^2
Fe	5.36	1.73E-7	12.43	**2.76E-5**	571	84.20	1.34E-7	62.46	**35.85**	**17.79**
Fe3%Cr	5.02	8.68E-7	8.12	**3.07E-5**	875	682.50	7.32 E-5	79.00	**70.80**	**13.14**
Fe5%Cr	12.03	3.12E-7	11.42	**2.77E-5**	853	251.65	1.34E-7	43.86	**37.36**	**23.45**

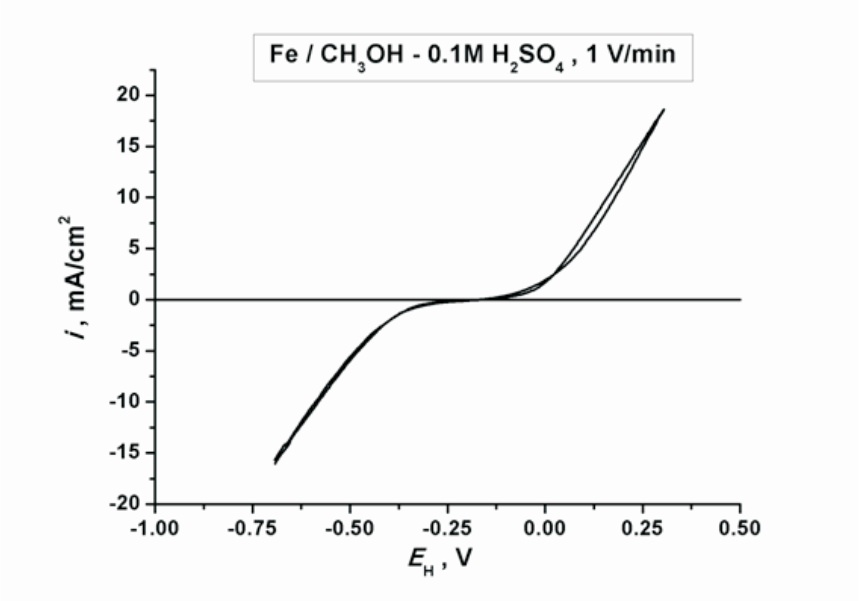

Fig. 2. Cyclic voltamperometric curves of iron in CH_3OH – 0.1M H_2SO_4 without *IR* correction

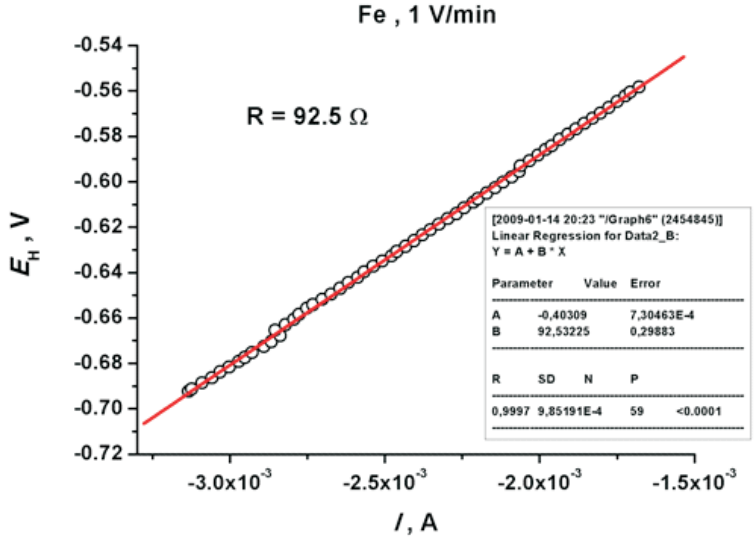

Fig. 3. Linear part of polarization curve used to calculate the resistance of electrolyte between Luggin capillary and working electrode

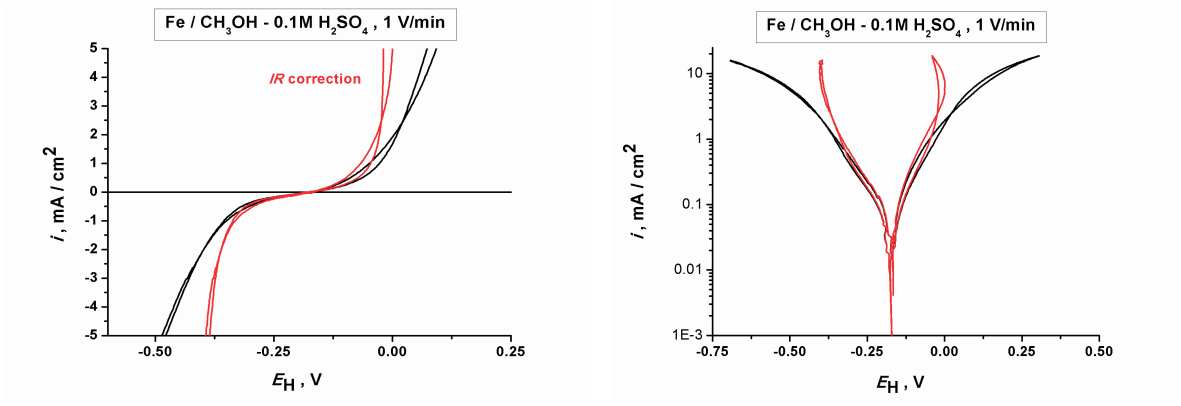

Fig. 4. Comparison of voltamperometric curves with and without *IR* correction in case of iron polarized in CH_3OH – 0.1M H_2SO_4 (a) in linear, (b) in semi -logarithm layout

3. Results and discussion

3.1. Voltamperometric measurements

Polarization curves of consecutive cycles except the first one are repeatable and illustrate anodic dissolution of metal and cathodic reduction of hydrogen ions. They characterize of distinct Tafel ranges both in anodic and cathodic branch. Fig. 5 shows the run of cyclic polarization curves for spectrally pure iron and for the Fe-1%Cr, Fe-3%Cr and Fe-5%Cr alloys.

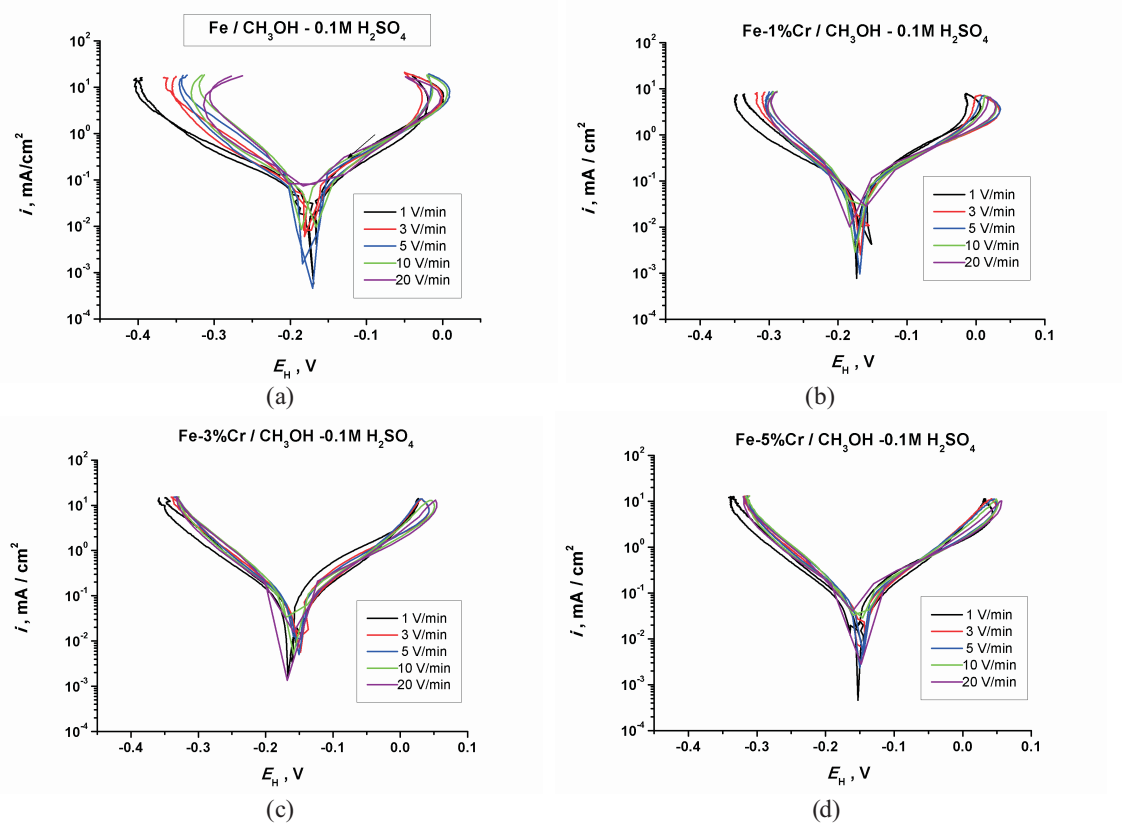

Fig. 5. Voltamperometric curves of iron and Fe-Cr alloys in CH_3OH – 0.1M H_2SO_4, (a) – spectrally pure iron, (b) – Fe-1%Cr, (c) – Fe-3%Cr, (d) Fe-5%Cr

3.1.1. Cathodic polarization

Cathodic polarization curves show hysteresis (Fig. 6 and 7) but Tafel slopes are similar for the curves leading into cathodic side and those returning. The influence of the scan rate on value b_c for the curve in cathodic direction and returning curve are presented in Fig. 8.

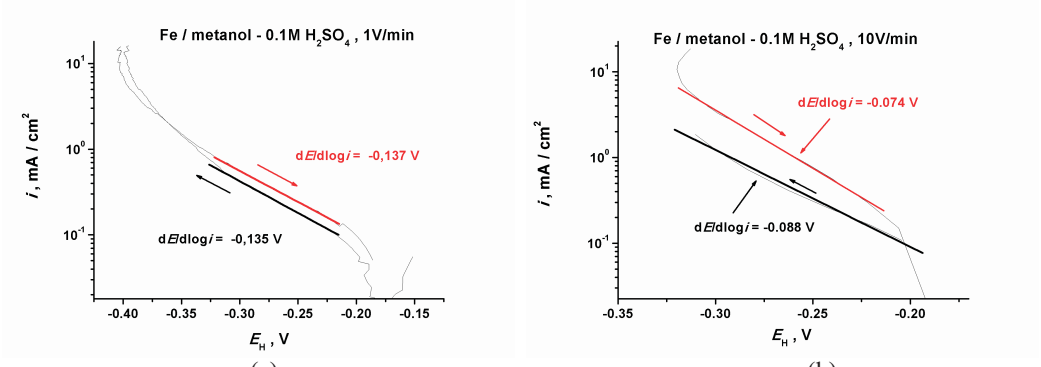

Fig. 6. Tafel plots of cathodic polarisation of iron in CH_3OH – 0.1M H_2SO_4 at the scan rate: (a) 1V/min and (b) 10V/min

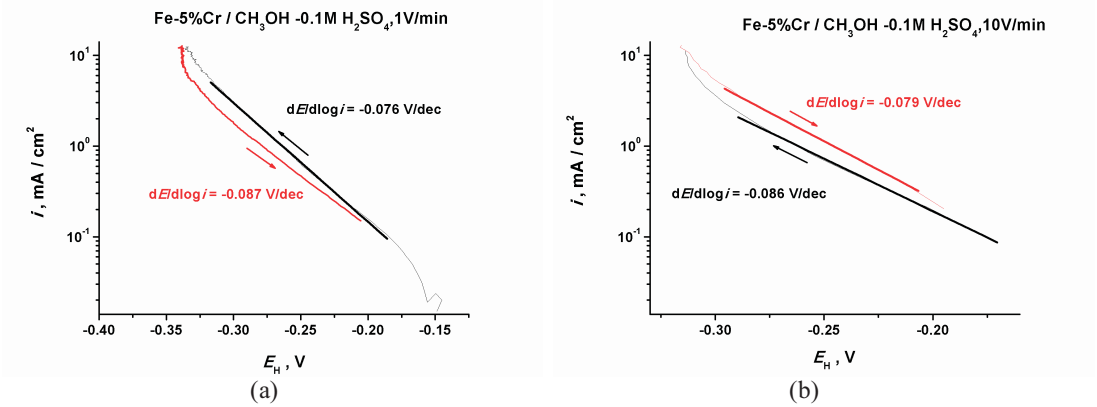

Fig. 7. Tafel plots of cathodic polarization of Fe-5%Cr alloy in CH_3OH – 0.1M H_2SO_4 at the scan rate: (a) 1V/min and (b) 10V/min

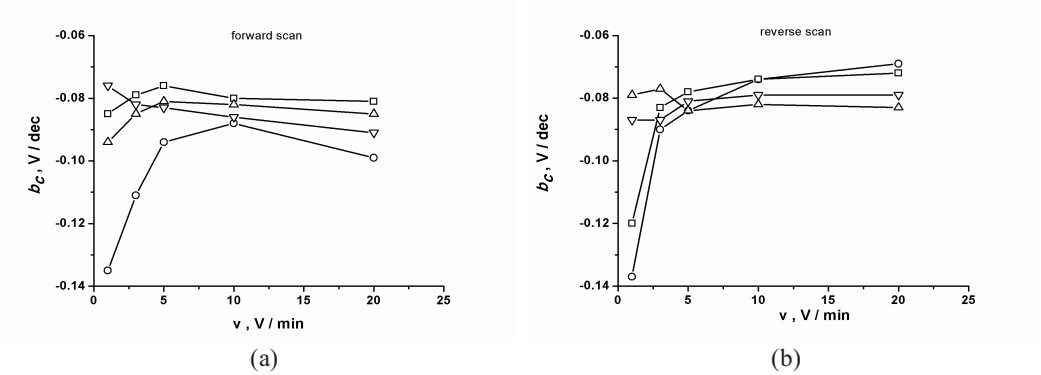

Fig. 8. The effect of the scan rate on the value of cathodic Tafel constant, (a) – curves from stationary potential in cathodic direction, (b) return curves (◇ – Fe, □ – Fe1Cr, Δ – Fe3cr, ∇ – Fe5Cr)

Alloys having 3 and 5% of chromium content have Tafel slope b_c in the range -0.07 to -0.09 V/dec, independent on scan rate. Pure iron and Fe-1%Cr alloy behave in a different way. At the higher speed of scanning they characterize by the lack of b_c relation on scan rate and Tafel slope similar to b_c value for the alloys having higher chromium content. Whereas at low scan rate $v < 5$ V/min, b_c has value close to -0.120 V/dec. The slope:

$$b_c = \frac{dE}{dlogi} = -2.3\frac{RT}{\alpha_c F} = -0.120V \qquad (1)$$

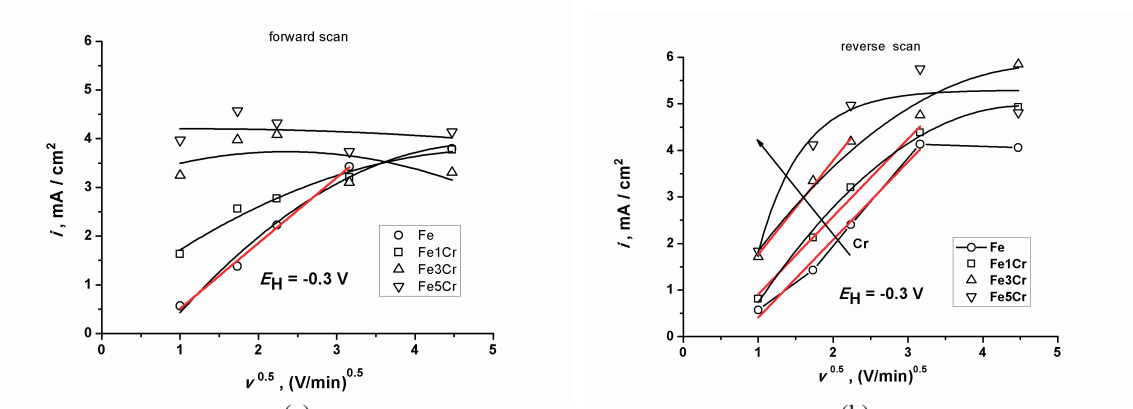

(a) (b)

Fig. 9. The effect of scan rate on current density at the potential -0.3V. (a) – values of polarization curves led in cathodic direction, (b) values of polarization curves led in anodic direction (return curve)

The influence of chromium on cathodic behavior of Fe-Cr alloys is marked by the increase of current density in the potential range of reduction of hydrogen ions (Fig. 8).

Analyses of presented above results of voltamperometric measurements proves that reduction of hydrogen ions from methanol solutions of sulphuric acid takes place on the iron surface according to Volmer - Heyrowski mechanism as it takes place in aqueous solutions:

$$H^+ + e \leftrightarrow H_{ad} \qquad (2)$$

$$H_{ad} + H^+ + e \rightarrow H_2 \qquad (3)$$

Heyrowski reaction (3) determines the rate of hydrogen evolution. At low scan rate (conditions similar to stationery ones) coverage Θ_{Had} is close to one thus b_c = -0.120V/dec (2.3RT/0.5F). At high v we have got $\Theta < 1$ and b_c reaches the value between -0.07 do -0.09 V/dec, close to Tafel slope b_c = -0.060V, corresponding to the process controlled by reaction (2) under condition of adsorption described by Temkin isotherm [20].

In the presence of chromium in the alloy Tafel slope reaches the value of about -0.080V already at lower scan rate. Chromium has higher bounding energy of M-H than iron and lower energy of electron escape [21] so it is the element stimulating reaction (2). It is unclear why Tafel slope b_c does not reach the value -0.120V for low scan rate (conditions close to stationery ones) in case of alloys containing chromium. Low Tafel slope for Fe-Cr alloys at these speeds can be explained by blocking of surface active places by adsorbed products of parallel reaction of anodic dissolution of chromium type $Cr(OCH_3)_2$. Degree of surface coverage Θ_{Had} will be then lower than one. At partial blocking of active places where the reaction (3) takes place it is possible to have partial participation of Tafel recombination reactions in the process of hydrogen evolution. Slope b_c between -0.07 to -0.09 V/dec can be the result of parallel Volmer-Heyrowski and Volmer-Tafel mechanisms.

3.1.2. Anodic polarization

In anodic range we have clear difference between curve led into positive potentials and return curve. Slope dE/dlog$i$ is lower for the curve in anodic direction than for the return curve. Clear hysteresis visible at high anodic over potentials is connected with surface activation

is typical for the hydrogen evolution in acid environment.

Fig 9 illustrates the influence of the scan rate on cathodic current density at the potential of -0.3V. In the range of low scan rate linear dependence of current density on $v^{0.5}$ proves diffusion control of reduction process of H^+ ions. At high scan rate current density takes constant value which may prove activation control of the process. The higher chromium content in the alloy the lower polarization scan rate is necessary for the change from diffusive to activation control.

by the removal of adsorption products. Fig. 10 and 11 illustrates the influence of scanning direction on the Tafel slope of polarization curves respectively for the pure iron and Fe-5%Cr alloy. Fig. 12 presents the effect of scan rate on the Tafel constant values b_a. It appears from diagrams in Fig. 12 a and b that b_a constant doesn't depend on the scan rate. It seems that the value calculated for the curve led in anodic direction (Fig.12a) is slightly higher than for the return curve (Fig.11b). Both values are close to the slope of b_a = 0.120 V, value corresponding to one electron reaction of the charge transfer. In water solutions of electrolytes iron has such Tafel slope only in case of total coverage of electrode by adsorbed $FeOH_{ad}$ – in the prepassive range [23]. In methanol solutions the metal surface will be covered by surface compound $M(OCH_3)_2$. Etching mechanism can be therefore described as follows:

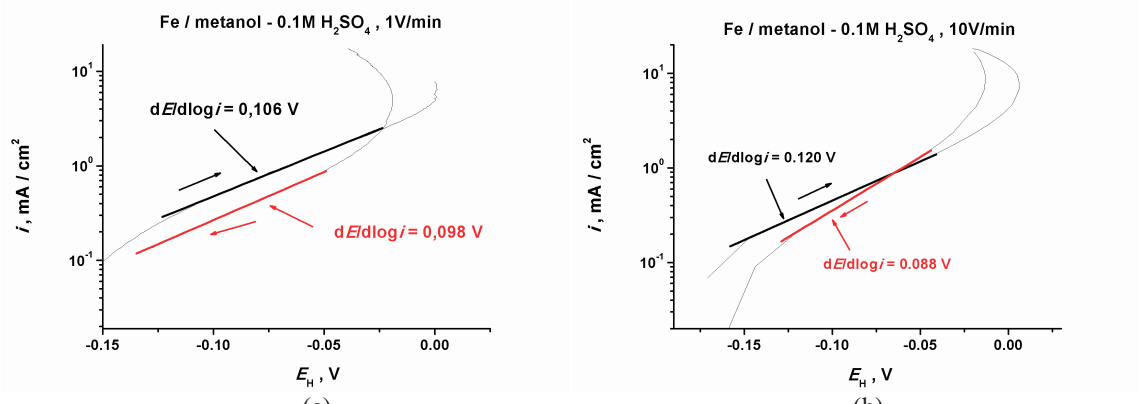

(a) (b)

Fig. 10. The influence of polarization direction on the Tafel slopes of voltamperometric curves for iron, (a) v = 1 V/min, (b) v = 10 V/min

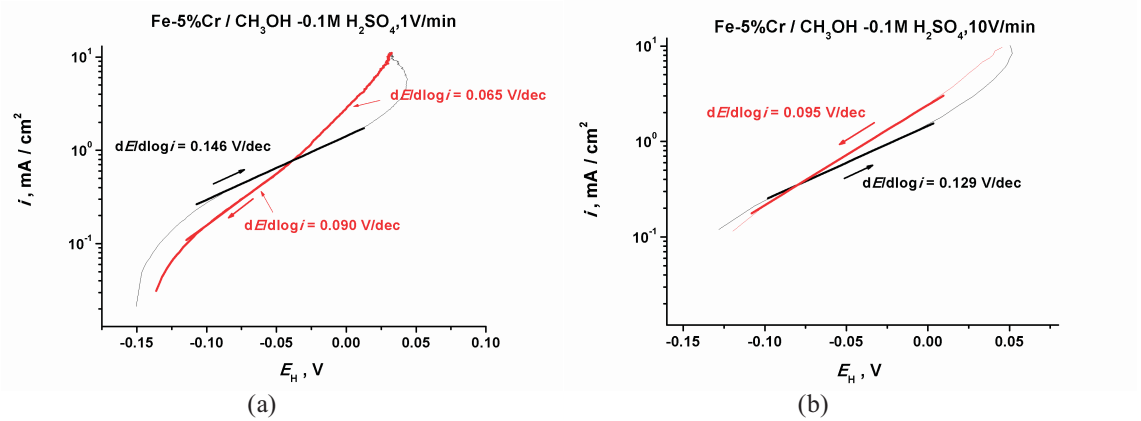

(a) (b)

Fig. 11. The influence of polarization direction on the Tafel slopes of voltamperometric curves for Fe-5%Cr alloy, (a) v = 1 V/min, (b) v = 10 V/min

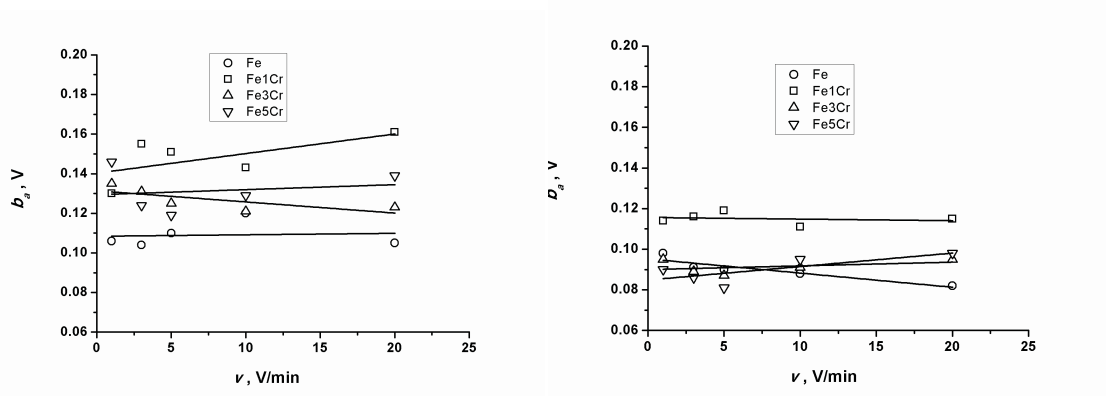

Fig. 12. The effect of scan rate on anodic Tafel constants values b_a, (a) – curves from stationary potential in cathodic and anodic direction, (b) return curves

$$M + CH_3OH \leftrightarrow MOCH_{3ad} + H^+ + e \qquad (4)$$

$$MOCH_{3ad} \rightarrow MOCH_3^+ + e \qquad (5)$$

Assuming that $\Theta_{MOCH3ad}$ equals one, b_a for this process is 0.120 V/dec.

3.1.3. Impedance measurements

Fig.13 a and b present Nyquist and Bode diagrams for pure iron and binary Fe-Cr alloys in anodic range at constant potential -0,03 V. Impedance spectrum in this range of potentials consists of three semicircles (Fig.13a). The first capacitive semicircle in the range of high frequencies can be attributed to *RC* of reference electrode unit (Fig. 14a) and also to *RC* connected with adsorption of a solvent – methanol (Fig. 14b). Faraday electrochemical process is described by the semicircle in the range of medium frequencies and flattened induction semicircle in the range of low frequencies. The diagrams present also simulation of impedance and shift of phase angle (full line) for the equivalent circuit *R(CR)(C(LR)(LR))*. Circuit diagram and its physical meaning is presented at Fig. 14 a and b. Table 2 presents the results of *R(RC)(C(LR)(LR))* circuit fitting to experimental results. In last two columns there is also added total resistance of charge transfer reaction $R_{ct} = R_1 \cdot R_2/(R_1 \cdot R_2)$ and total electrolyte resistance $R_{e1} + R_{e2}$ (for14a variant). Inductive loop visible in all diagrams proves that anodic reaction takes place with the presence of surface intermediate product. Taking into consideration that we have to do with the dissolution of two alloy components according to the reactions:

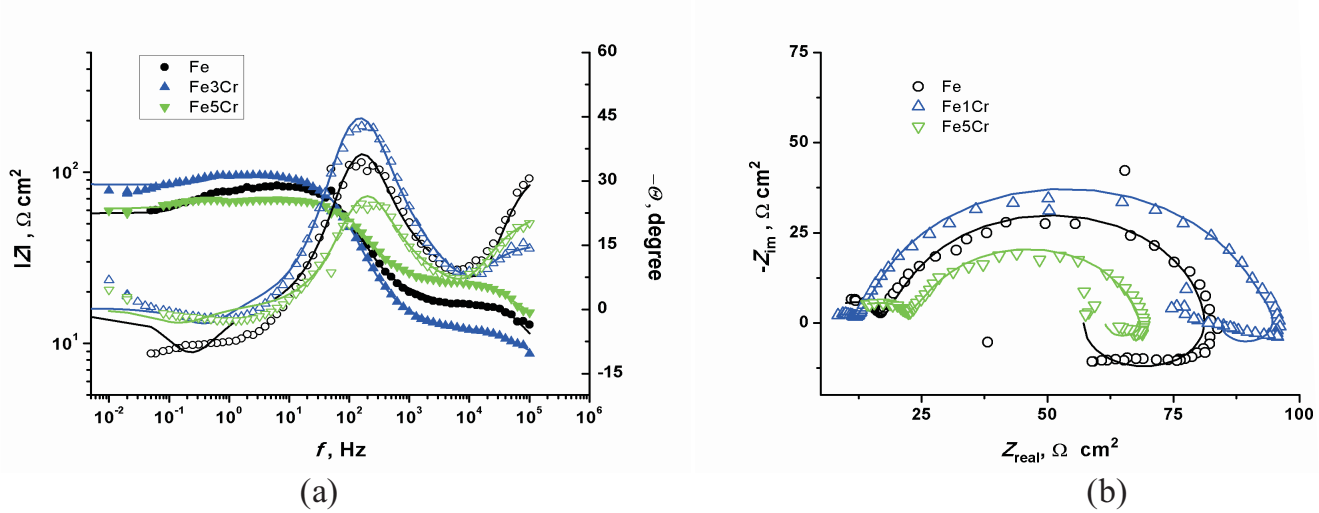

Fig. 13. Nyquist (a) and Bode diagram (b) for iron and Fe-Cr alloys in CH_3OH-0.1M H_2SO_4 at constant potential E_H = -0.03 V

$$Fe \rightarrow Fe^{+}_{ad} \rightarrow Fe^{2+} \qquad (6)$$

$$Cr \rightarrow Cr^{+}_{ad} \rightarrow Cr^{2+} \qquad (7)$$

equivalent circuit, presented on Fig.14 has been suggested. It consists of two *LR* elements related to reaction (6) and (7) and integrated with the adsorption of surface intermediates.

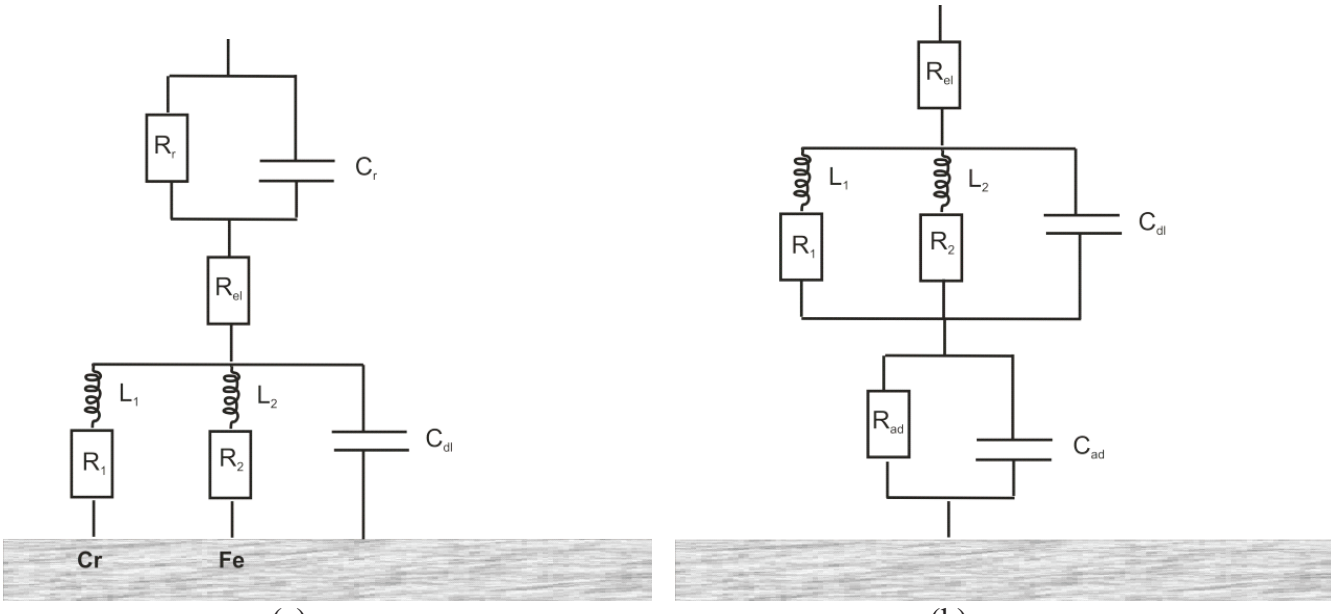

Fig. 14. Equivalent circuit *R(RC)(C(LR)(LR))* for impedance diagrams presented at Fig. 13, (a) *RC* high – frequency element is connected with the circuit of reference electrode, (b) *RC* high – frequency element exemplifies electrosorption of the solvent

Presented analyses of impendence spectrums of iron and Fe-Cr alloys shows that there aren't any significant differences in mechanism and kinetics of anodic dissolution of these alloys. Both the capacity of double layer C_{dl} and the resistance of charge transfer R_{ct} are similar and there is a lack of any clear tendency of changing those parameters together with the increase of chromium concentration in the alloy.

3.1.4. Corrosion potential and corrosion rate

Fig. 15 and 16 present the influence of chromium content in Fe-Cr alloys on the value of corrosion potential E_{corr} and corrosion current i_{corr} taken from the analyses of voltamperometric curves, at the scan rate of 1 V/min. The value of corrosion current has been calculated by Stern and Geary method [24] and by extrapolation of Tafel slopes (Fig.17).

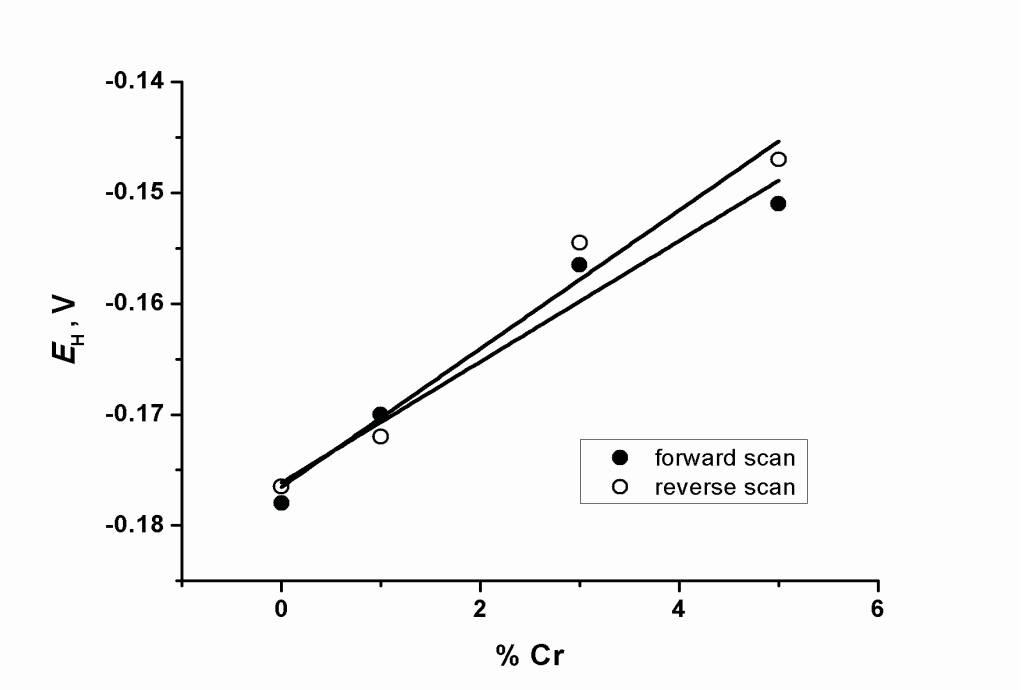

Fig. 15. The influence of chromium content on the corrosion potential of Fe-Cr alloy in CH_3OH – 0.1M H_2SO_4 solution , (v = 1 V/min)

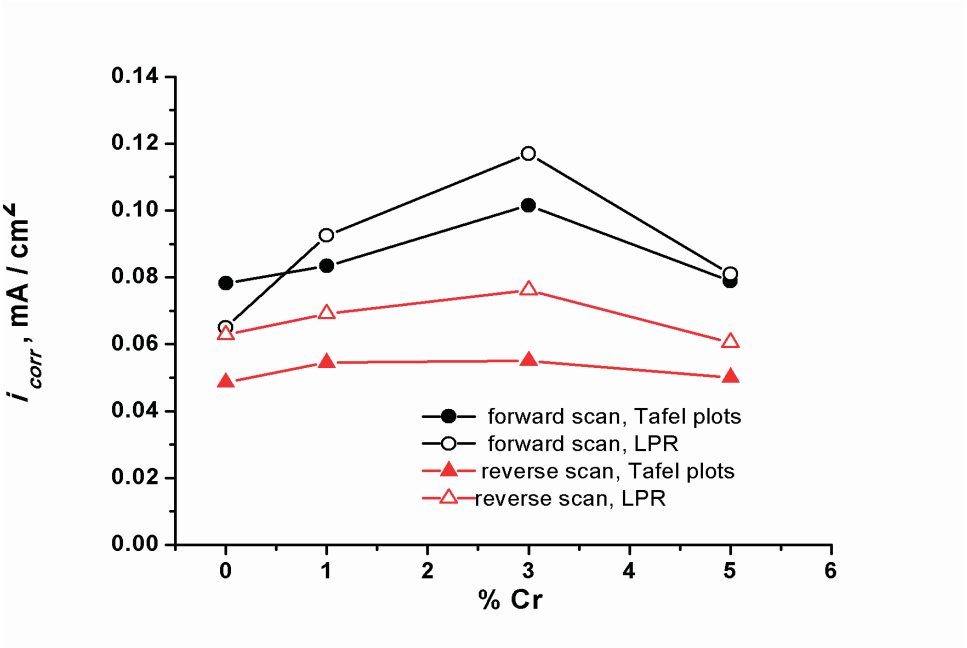

Fig. 16. The influence of chromium content on the of corrosion current density of Fe-Cr alloy in CH_3OH – 0.1M H_2SO_4 solution, (v = 1 V/min)

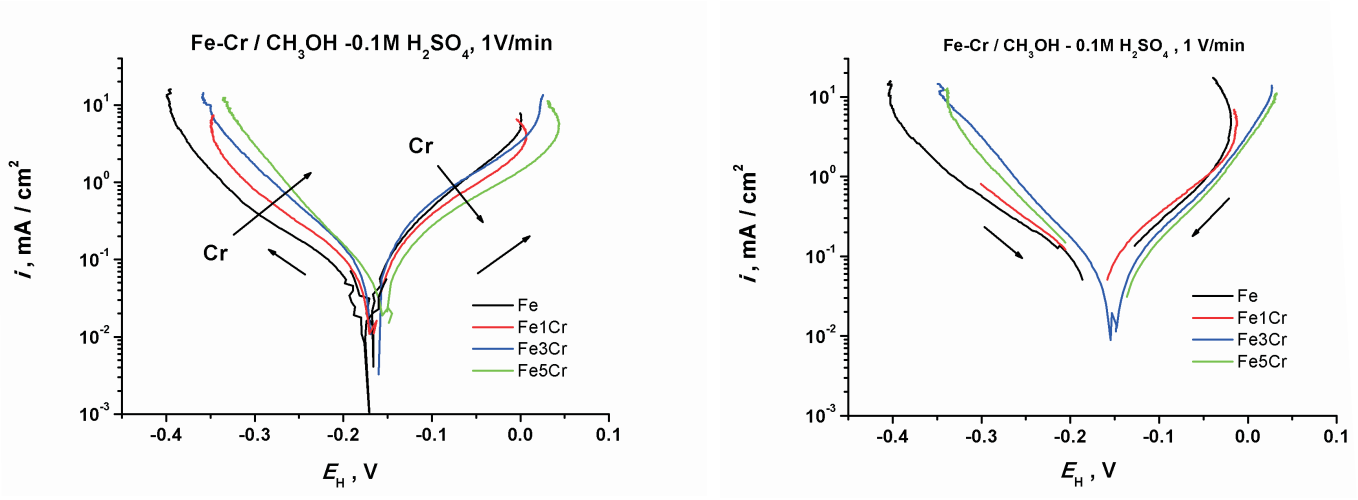

Fig. 17. The influence of the chromium content on polarization of Fe-Cr alloys in CH_3OH – 0.1M H_2SO_4, (a) – curves from stationary potential in cathodic and anodic direction, (b) return curves

Stationary potential grows significantly with the increase of chromium concentration. The influence of chromium content on the density of corrosion current is minimal because of opposite effect of this element on anodic and cathodic curves (stimulation of hydrogen reaction, inhibiting of anodic reaction), visible on Fig.16.

4. Conclusions

Mechanism of corrosion of iron and low – chromium Fe-Cr alloys in CH_3OH – 0.1M H_2SO_4 solution can be described by consecutive anodic process with the participation of mintermediate product (reactions 4 and 5) and cathodic reduction of hydrogen ions.

The presence of inductive loop in EIS spectrum in anodic range and hysteresis of LSV curves prove the participation of intermediate surface products in anodic reaction.

The presence of chromium in Fe-Cr solid solution affects the mechanism and kinetics of cathodic reduction of hydrogen ions. Already little amount of chromium (to 5wt%) increases the rate of hydrogen evolution and shifts the corrosion potential of alloy in anodic direction. The mechanism of cathodic reaction changes from Volmer–Heyrowski mechanism for pure iron to mixed Volmer–Heyrowski and Volmer-Tafel mechanism for Fe-Cr alloys. This change is probably connected with blocking of active places (kinks, steps) in which reaction (3), with participation of $CrOCH_3$ product, takes place. This results in the displacement of hydrogen recombination reaction to the surface where Tafel recombination can dominate (terraces).

Blocking of active places by $CrOCH_{3ad}$ intermediate product causes increase of overpotential of anodic reaction. Inhibition of anodic dissolution of the alloy is visible in LSV measurements (decrease of anodic current together with the increase of chromium concentration in ferrite).

The increase of chromium content in Fe-Cr alloys up to 5wt% has a little influence on corrosion rate which is the result of two parallel overlapping effects: stimulation of hydrogen reaction and inhibition of anodic process.

Acknowledgements

The work was supported by Polish Ministry of Science and Higher Education, AGH project 11.11.170.318.

REFERENCES

[1] J. Banaś, Z. Phys. Chem. **262**, 6, 1105 (Leipzig, 1982).
[2] J. Banaś, Electrochim. Acta **32**, 6, 871 (1987).
[3] J. Banaś, Materials Science Forum **185-188**, 845 (1995).
[4] J. Banaś, B. Mazurkiewicz, W. Solarski, K. Banaś, Materials Science Forum **185-188**, 871 (1995).
[5] S. Sternberg, V. Brânzoi, Electrochim. Acta **29**, 1, 15 (1984).
[6] F. Mazza, S. Torchio, N. Ghislandi, Int. Congress on Metallic Corrosion **1** 465 ed. National research Council of Canada, Ottawa (1984).
[7] P. L. de Anna, Corr. Sci, 25, 43 (1985).

[8] F. Belucci, G. Capobianco, G. Faita, C. A. Farina, G. Farina, F. Mazza, S. Torchio, Corr. Sci. **28**, 371 (1988).
[9] C. S. Brossia, E. Gileadi, R. G. Kelly, Corr. Sci. **17**, 9, 1455 (1995).
[10] M. Sakakibara, N. Saito, H. Nishihara, K. Arami, Corr. Sci. **34** (1993) 391.
[11] J. Banaś, B. Stypuła, K. Banaś, J. Świątowska-Mrowiecka, M. Starowicz, U. Lelek-Borkowska, Journal of Solid State Electrochemistry, in press, "on line acess: DOI.10. 1007/s 10008-008-0649.5".
[12] M. Sakakibara, H. Nishihara, K. Arami, Corr. Sci. 34 (1993) 1937.
[13] Ya. Kolotyrkin, G. G. Kossyj, Zassch. Metall. **1**, 252 (1965).
[14] J. Banaś, Electrochim. Acta **27**, 8, 1141 (1982).
[15] J. Banaś, Electrochim. Acta **27**, 1, 71 (1982).
[16] B. Stypuła, J. Banaś, Electrochim. Acta **38**, 15, 2309 (1993).
[17] J. Banaś, B. Mazurkiewicz, B. Stypuła, Electrochim. Acta **37**, 6, 1069 (1992).
[18] J. Banaś, B. Mazurkiewicz, B. Stypuła, ACH Models in Chemistry **132**, 4, 607 (1995).
[19] A. I. Vogel, Preparatyka organiczna, WNT 1984.
[20] E. Gileadi, B. E. Conway, in Modern Aspects of Electrochemistry, J. O'M. Bockris and B. E. Conway, Eds., Butterwoths, London, 1964, Chapter 5.
[21] S. Trasatti, J. Electroanal. Chem. **39**, 163 (1972).
[22] A. Belanger, Ashok K. Vijh, J. Electrochem. Soc. 121,2,225 (1974).
[23] W. J. Lorenz, K. E. Heusler, Anodic Dissolution of Iron Group Metals, in Corrosion Mechanisms ed. by F. Mansfeld, Marcel Dekker Inc. N.York-Basel, 1987.
[24] M. Stern, A. L. Geary, J. Electrochem. Soc. **104**,1,56 (1957).

Received: 10 May 2009.